

Supporting Information

Polymer Additive-Promoted Porous  $\text{PbBr}_2$  Layer for Fabricating High-Performance

Carbon-Based  $\text{CsPbIBr}_2$  Perovskite Solar Cells through a Two-Step Sequential

Deposition Process

Guiqiang Wang, Jiarun Chang, Dongsheng Wang, Jiayu Bi, Fanning Meng

School of chemistry and Materials, Bohai University, Jinzhou 121003

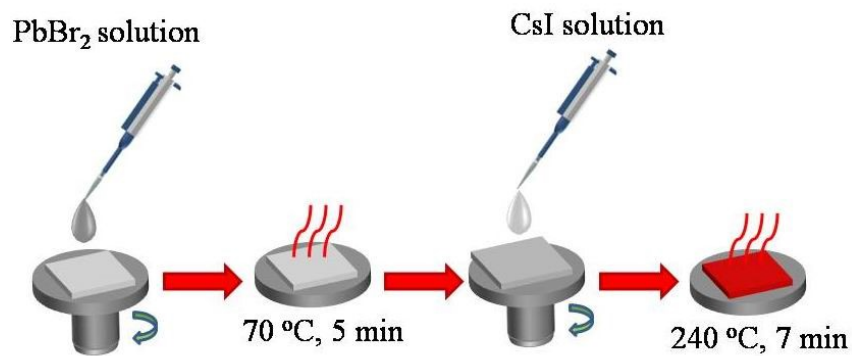


Fig. S1 Schematic illustration of the fabrication process of CsPbIBr<sub>2</sub> perovskite film through a two-step sequential deposition process.

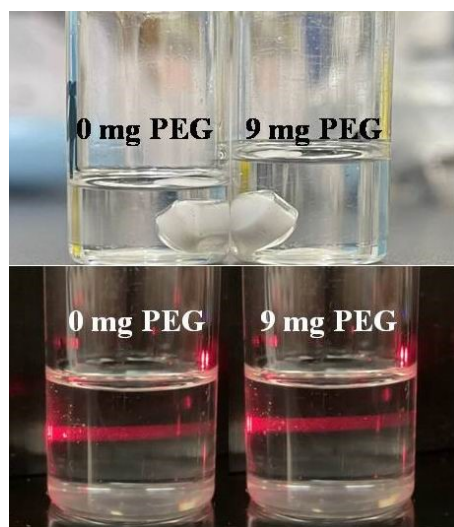


Fig. S2 Photographs of PbBr<sub>2</sub> solution without and with 9 mg PEG and their Tyndall effect

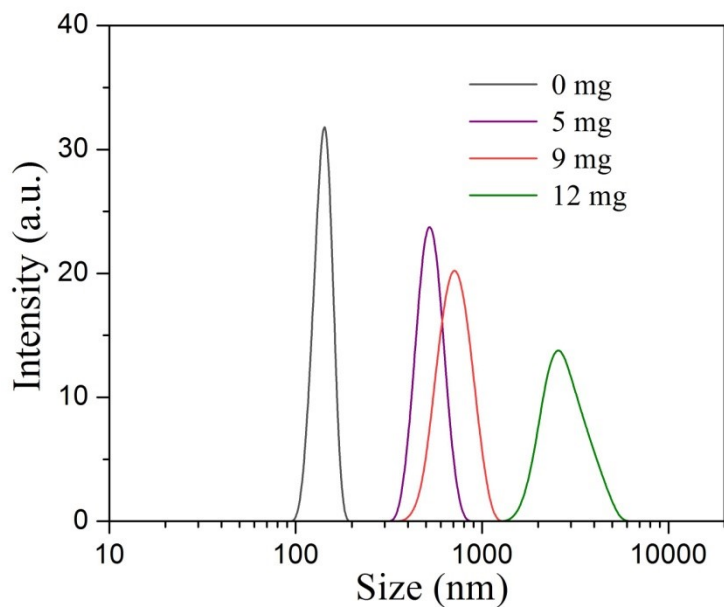


Fig. S3 Size distributions of  $\text{PbBr}_2$  colloidal particles in the solution with different amounts of PEG detected by dynamic light scattering.

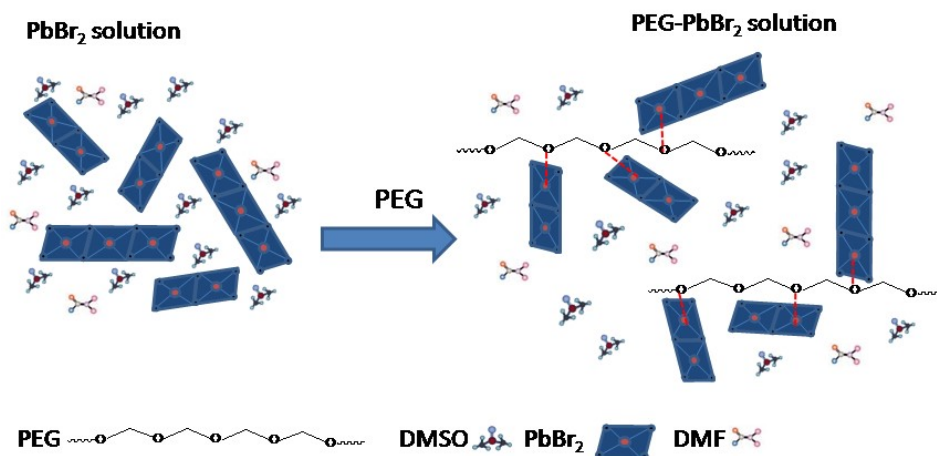


Fig. S4 Schematic process of  $\text{PbBr}_2$  colloid aggregation induced by PEG additive

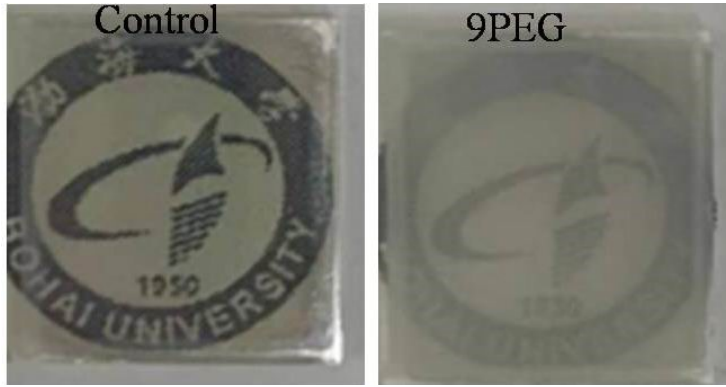


Fig. S5 Photographs of  $\text{PbBr}_2$  film deposited on FTO/ $\text{TiO}_2$  substrate without and with 9 mg PEG

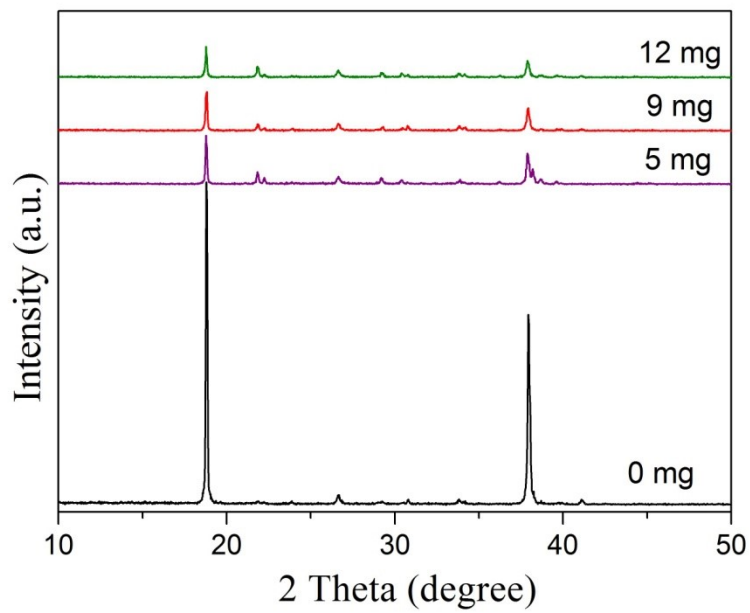


Fig. S6 XRD curves of  $\text{PbBr}_2$  film with different amounts of PEG

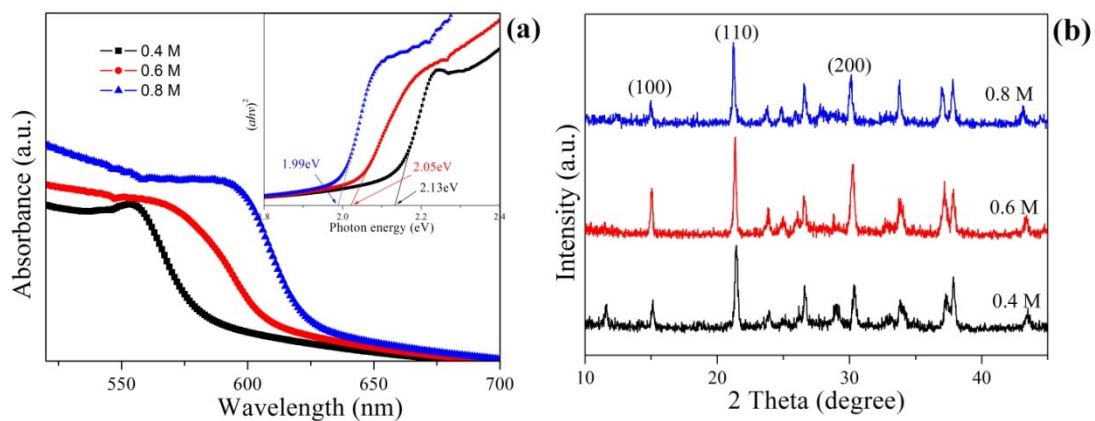


Fig. S7 (a) UV-vis absorption spectra and (b) XRD curves of CsPbI<sub>2</sub>Br<sub>2</sub> perovskite obtained from CsI solution with different concentrations.

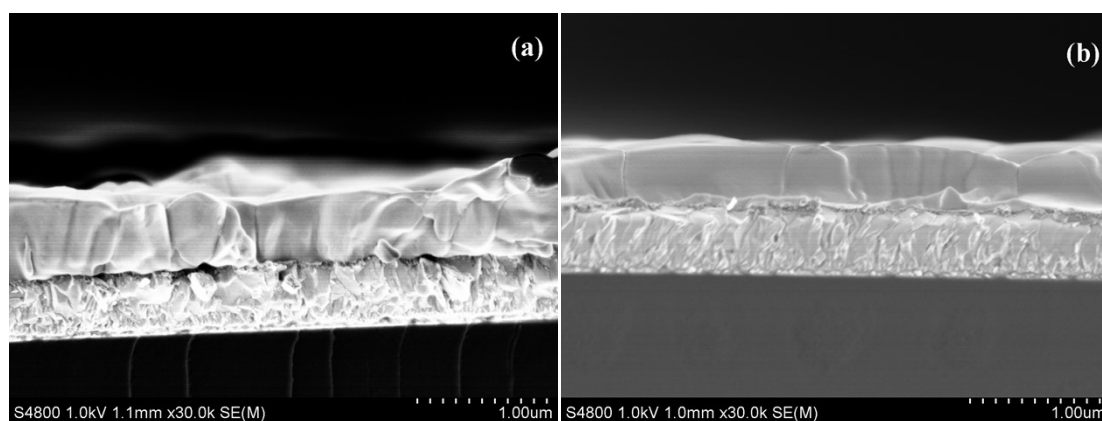


Fig. S8 Cross-sectional SEM images of the control (a) and 9PEG (b) CsPbI<sub>2</sub>Br<sub>2</sub> perovskite films

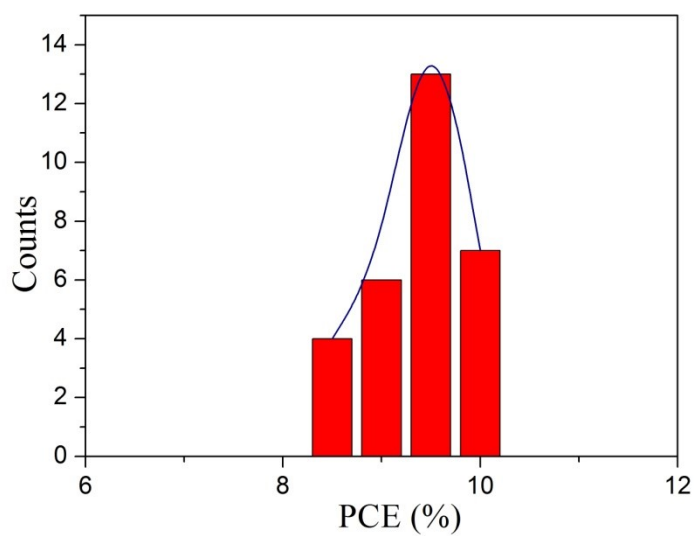


Fig. S9 The statistical PCEs of 30 independent cells based on 9PEG CsPbIBr<sub>2</sub> perovskite film.

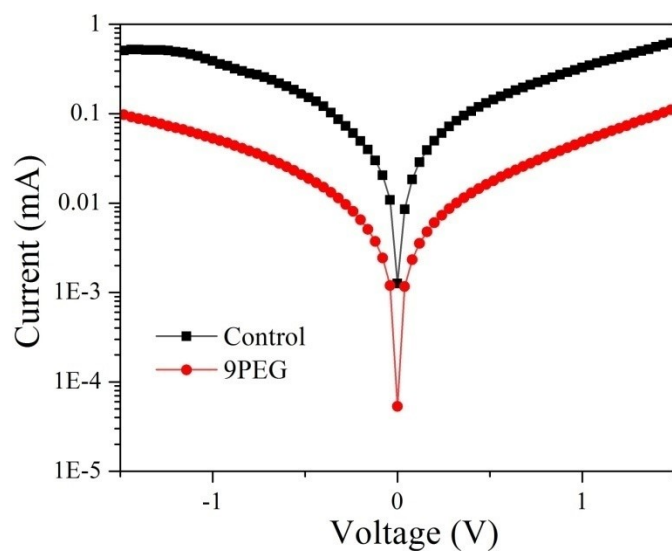


Fig. S10 Dark current density-voltage curves of the devices based on the control and 9PEG CsPbIBr<sub>2</sub> perovskite films

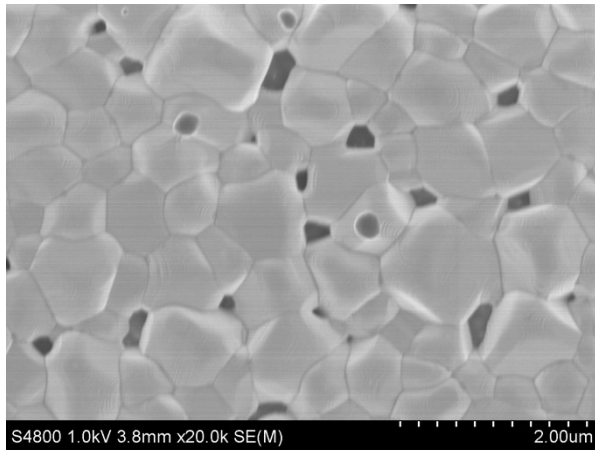


Fig. S11 SEM image of CsPbIBr<sub>2</sub> perovskite film obtained by one-step solution process